

See discussions, stats, and author profiles for this publication at: <https://www.researchgate.net/publication/243659308>

# EDTA and CN – Complexing Effect on the Kinetics, Spectral Properties, and Redox Properties of Ag<sup>10</sup> and Ag<sup>2+</sup> in Aqueous Solution

ARTICLE *in* THE JOURNAL OF PHYSICAL CHEMISTRY · JUNE 1996

Impact Factor: 2.78 · DOI: 10.1021/jp960176g

---

CITATIONS

25

---

READS

16

3 AUTHORS, INCLUDING:



**Samy Remita**

Conservatoire National des Arts et Métiers

53 PUBLICATIONS 645 CITATIONS

SEE PROFILE



**Mehran Mostafavi**

Université Paris-Sud 11

162 PUBLICATIONS 2,910 CITATIONS

SEE PROFILE

# EDTA and CN<sup>−</sup> Complexing Effect on the Kinetics, Spectral Properties, and Redox Properties of Ag<sub>1</sub><sup>0</sup> and Ag<sub>2</sub><sup>+</sup> in Aqueous Solution

S. Rémita, M. Mostafavi,\* and M. O. Delcourt

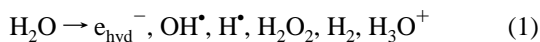
Laboratoire de Physico-Chimie des Rayonnements, CNRS (URA 75), Université Paris-Sud, Bâtiment 350, 91405 Orsay Cedex, France

Received: January 19, 1996; In Final Form: April 2, 1996<sup>⊗</sup>

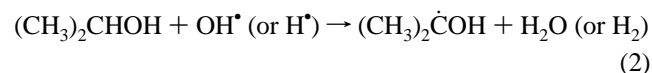
The first steps of silver clusters nucleation have been studied by pulse radiolysis in the presence of EDTA and CN<sup>−</sup> ligands. The successive rate constants and the transient absorption spectra corresponding to Ag<sub>1</sub><sup>0</sup> and Ag<sub>2</sub><sup>+</sup> have been determined. It has been found that Ag<sub>1</sub><sup>0</sup> and Ag<sub>2</sub><sup>+</sup> were complexed by the ligands. In addition to the usual charge-transfer-to-solvent (CTTS) bands, red shifted in the presence of EDTA and CN<sup>−</sup>, the complexed Ag<sub>1</sub><sup>0</sup> and Ag<sub>2</sub><sup>+</sup> spectra exhibit an additional absorption band assigned to a metal-ligand-charge-transfer (MLCT). The red shift of the CTTS band of the silver atom, which is more pronounced when the ligand interaction is stronger, is correlated with the ligand-induced redox properties of the monomeric silver couple.

## Introduction

Spontaneous evolution of the silver atoms produced by a short pulse of ionizing radiation in a solution containing free hydrated silver ions was studied in detail previously,<sup>1–7</sup> and most of the kinetic data are available. It is well-known that the ionizing irradiation in such a silver solution generates the following various radiolytic species from the water solvent:

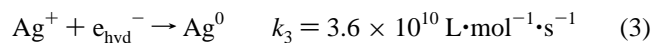


In the presence of an alcohol such as 2-propanol (CH<sub>3</sub>)<sub>2</sub>CHOH, OH<sup>•</sup> and H<sup>•</sup> radicals are scavenged to produce a reducing (CH<sub>3</sub>)<sub>2</sub>ĊOH radical:

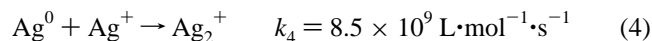


Under these conditions the short-lived transient species are solvated electrons (the radiolytic yield, *G*, amounts to 2.7 per 100 eV) and (CH<sub>3</sub>)<sub>2</sub>ĊOH (*G* = 3.3).

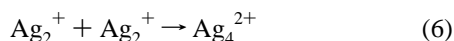
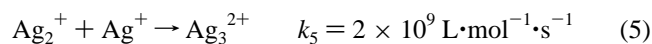
The scavenging reaction of e<sub>hyd</sub><sup>−</sup> by the silver ion<sup>8</sup>



is followed by the complexation with another silver ion:<sup>7</sup>



After this step, the coalescence starts with the following reactions:<sup>7</sup>



Then generally we can summarize all coalescence reactions as below:



For free clusters in aqueous solution, in the absence of ligands and polymers, the aggregation process does not cease before high values of *n* are attained (leading to the colloid and even the precipitate). However, the environment determining the properties of a cluster can include, in addition to the solvent, a surfactant or a complexing agent which slows down or even stops the aggregation process at an earlier stage. Indeed, we have shown, recently, a drastic slowing of the aggregation process in the presence of polyacrylate (PA), and the stabilization of a few well-defined oligomer clusters with a nuclearity *n* lower than 8–10.<sup>9–15</sup> It was concluded that the carboxylate groups COO<sup>−</sup> of the PA complex silver ions and small clusters very efficiently.<sup>9–13</sup> Pulse radiolysis experiments have shown that the nature of the earliest clusters is similar to that obtained in the absence of PA; however the spectra exhibit an additional absorption band which indicates that the species are complexed.<sup>14</sup>

It is interesting to understand the influence of the complexation on the spectral properties of the clusters in solution. In a free aqueous medium, the absorption spectrum of Ag<sub>1</sub><sup>0</sup><sup>2,3,7</sup> consists of a single absorption band centered at 360 nm which has been shown to be a charge-transfer-to-solvent (CTTS) band; its maximum depends on the solvent and on temperature.<sup>16–18</sup> However, the transient Ag<sub>1</sub><sup>0</sup>(NH<sub>3</sub>)<sub>2</sub> presents a red shifted spectrum which contains more than a single absorption band. The presence of additional bands, as in the case of PA, bears witness to the interaction between the silver atom and NH<sub>3</sub> ligands.<sup>19</sup>

On the other hand, it is also interesting to understand the influence of ligands, *L*, on the redox potential of the monomer couple, Ag<sub>1</sub><sup>1</sup>L/Ag<sub>1</sub><sup>0</sup>L, which concerns the first step of the nucleation. The first estimations of such a redox potential were carried out very recently in the case of silver monomer couple complexed by cyanide<sup>20</sup> and ammonia.<sup>19</sup> The redox potential of the Ag<sub>1</sub><sup>+</sup>/Ag<sub>1</sub><sup>0</sup> couple in aqueous solution (−1.75 V<sub>NHE</sub>) is significantly decreased by the ammonia and cyanide ligands down to −2.4 and −2.6 V<sub>NHE</sub>, respectively. These two estimations were also confirmed by radiolysis experiments.<sup>19,21</sup>

The aim of the present study is to determine the influence of two anionic ligands, ethylenediaminetetraacetate (EDTA) and

\* To whom correspondence should be addressed.

⊗ Abstract published in *Advance ACS Abstracts*, May 15, 1996.

cyanide, on the formation kinetics and the spectra of the first silver clusters. Then we will try to correlate the ligand-induced spectral properties of the complexed atom with its redox properties.

## Experimental Section

All the reagents were pure chemicals used as purchased:  $\text{KAg}(\text{CN})_2$  from CLAL,  $\text{Ag}_2\text{SO}_4$  from Fluka, 2-propanol (2-PrOH) and NaOH from Prolabo, and EDTA from Aldrich. Solutions containing  $\text{Ag}^+$  and  $\text{Ag}(\text{CN})_2^-$  were prepared by dissolution of the two salts  $\text{Ag}_2\text{SO}_4$  and  $\text{KAg}(\text{CN})_2$  and carefully stored in the dark before use. EDTA (denoted  $\text{H}_4\text{Y}$ ) can present up to four  $\text{COO}^-$  binding groups depending on the pH of the solution. The  $\text{Ag}^+$  ions are known to be complexed with the deprotonated ethylenediaminetetraacetate  $\text{Y}^{4-}$  form of EDTA, thus leading to the complex  $\text{AgY}^{3-}$  (stability constant  $10^{7.3}$ ).<sup>22</sup> In order to prepare silver ions complexed by  $\text{Y}^{4-}$ , we have kept the solution basic ( $\text{pH} \approx 10$ ) and the initial ratio  $[\text{EDTA}]/[\text{Ag}^+]$  constant at 5. Taking into account all the equilibria (complexation and acidity), the ratio  $[\text{AgY}^{3-}]/[\text{Ag}^+]$  is found to be  $10^{4.5}$  at  $\text{pH} = 10$  when the initial concentration of EDTA is  $5 \times 10^{-3}$ , so that  $\text{AgY}^{3-}$  is the dominant form under the conditions used.<sup>23</sup>

Electron pulses (3 ns duration) were delivered by a Febetron 706 (600 keV electron energy) to samples contained in a silica cell with a thin entrance window (0.2 mm) and an optical path length of 1 cm. The cell was deaerated by a nitrogen flow; the solution was changed after each pulse to prevent possible reactions with long-lived clusters. Typical reducing transient concentrations were in the range of  $10^{-5}$ – $10^{-4}$  mol·L<sup>-1</sup>. Absorption of transient species was analyzed by means of a classical xenon lamp, monochromator, and photomultiplier assembly. The splitting of the beam allows the signals to be recorded simultaneously at two different wavelengths. The electron decay is then observed at the reference wavelength 550 nm.

The kinetics of the reduction of  $\text{CN}^-$  by the hydrated electron  $e_{\text{hyd}}^-$  has already been studied by pulse radiolysis: the rate constant of this reaction was found to be  $3 \times 10^5$  L·mol<sup>-1</sup>·s<sup>-1</sup>.<sup>24</sup> The kinetics of the reduction of EDTA by  $e_{\text{hyd}}^-$  has also been studied by pulse radiolysis as a function of pH.<sup>25</sup> The rate constant of this reaction decreases when the pH increases. Its order of magnitude is roughly  $10^6$  L·mol<sup>-1</sup>·s<sup>-1</sup> in basic medium and less than  $10^8$  L·mol<sup>-1</sup>·s<sup>-1</sup> in acidic medium.<sup>25</sup> The kinetics of the reduction of  $\text{CN}^-$  and  $\text{Y}^{4-}$  is thus very slow in comparison with the reduction of silver ions by hydrated electrons, so that these two reactions could be neglected in our experiments.

## Results

**I.  $\text{CN}^-$  Complexing Effect. Transient Spectra.** Figure 1 shows the spectra obtained at four times after the pulse in a  $\text{Ag}(\text{CN})_2^-$  solution: 100, 200, 300, and 900 ns, chosen as kinetically marking steps, as can be seen in Figures 2 and 3. At 100 ns, on the red side of the spectrum, the broad band of the hydrated electron  $e_{\text{hyd}}^-$  is clearly present while two bands have appeared peaking at 450 and 500 nm (Figure 2). Other bands are present in the range 250–400 nm which continue to increase after 100 ns (Figure 1).

At 200 ns, the absorption of the hydrated electron has partly faded. The bands at 450 and 500 nm are still present, the absorption at 350 nm has grown, and a shoulder has appeared at 410 nm (Figure 1).

At 300 ns, the two bands at 450 and 500 nm have decreased together. The band at 350 nm has attained its maximal value

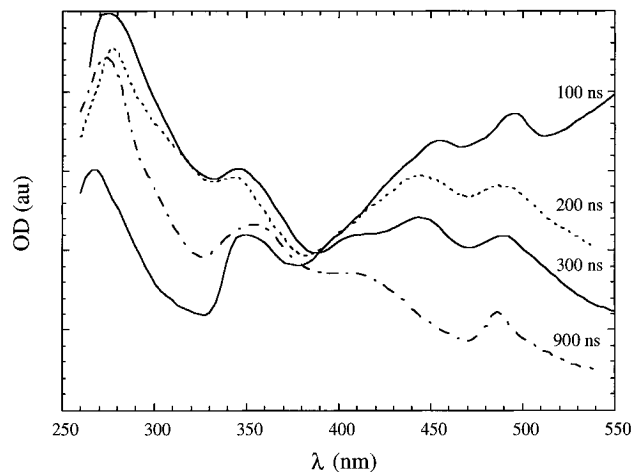


**Figure 1.** Spectra obtained by pulse radiolysis of a solution containing  $[\text{Ag}(\text{CN})_2^-] = 10^3$  mol·L<sup>-1</sup>, and  $[\text{2-propanol}] = 0.2$  mol·L<sup>-1</sup>, 100, 200, 300 and 900 ns after the pulse. The pH was adjusted at 10.

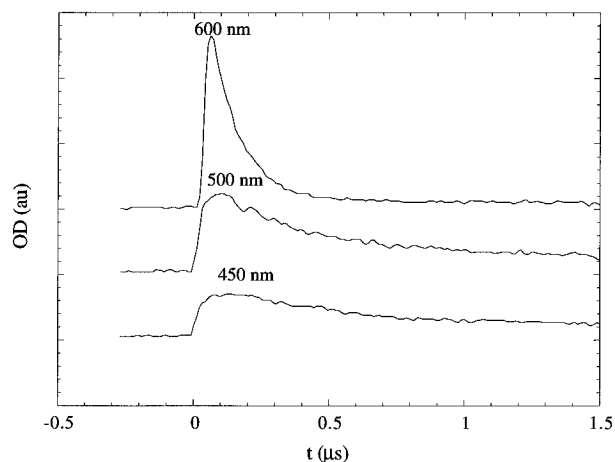


**Figure 2.** Time profile of the absorption at 600, 500, and 450 nm. Same conditions as Figure 1.

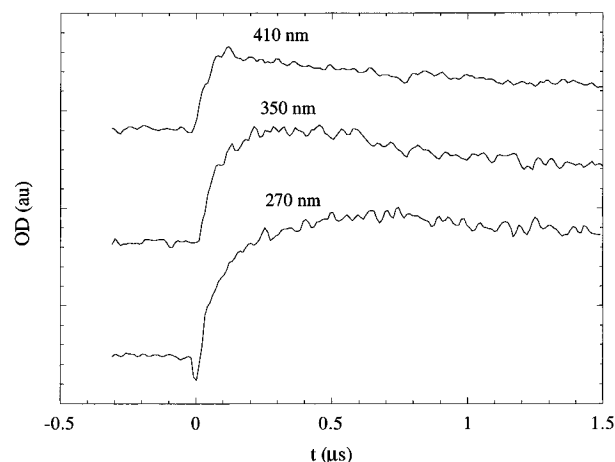


**Figure 3.** Time profile of the absorption at 410, 350, and 270 nm. Same conditions as Figures 1 and 2.

(Figure 3) while the absorption at 410 nm appears clearly to be a new band (Figure 1).

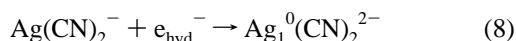
After 300 ns, in addition to the 270 nm absorption band which increases up to 700 ns (Figure 3), the spectrum displays three bands (350, 410, and 490 nm) which decrease together (Figure 1).

**Kinetic Steps.** The reduction of  $\text{Ag}(\text{CN})_2^-$  by  $e_{\text{hyd}}^-$  at pH 10 has already been studied by Anbar et al.<sup>26</sup> Working with an excess of cyanide ligands, the authors found a rate constant

of  $1.5 \times 10^9 \text{ L}\cdot\text{mol}^{-1}\cdot\text{s}^{-1}$ . A more complete study of this reduction, versus the concentration of complexed metal ions, has recently yielded the value  $5 \times 10^9 \text{ L}\cdot\text{mol}^{-1}\cdot\text{s}^{-1}$ .<sup>27</sup>

In order to distinguish more clearly the successive reactions, the time profile of absorbances has been plotted in Figures 2 and 3 for typical wavelengths: over the first 300 ns, two main kinetic steps can be seen which are then followed by others.

**First Step 0–100 ns.** At 600 nm, the initial absorption, due to  $e_{\text{hyd}}^-$ , decays according to pseudo-first-order kinetics while the 450 and 500 nm peaks appear (Figure 2). The two wavelengths 450 and 500 nm are the absorption maxima of the species formed during the decay of  $e_{\text{hyd}}^-$ . The time evolution of the spectrum shows that no species displays a maximal absorption at 360 nm (Figure 1). We conclude that the product of the reduction of  $\text{Ag}(\text{CN})_2^-$  by the hydrated electron, as has been predicted by a previous theoretical calculation,<sup>20</sup> is the complexed atom  $\text{Ag}_1^0(\text{CN})_2^{2-}$  and not the free silver atom  $\text{Ag}_1^0$  (which absorbs at 360 nm), according to the following reaction:

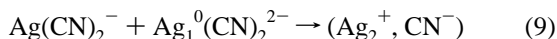


At 450 and 500 nm, the  $e_{\text{hyd}}^-$  absorption cannot be neglected so that the corresponding kinetics signals of Figure 2 are a combination of the disappearance of  $e_{\text{hyd}}^-$  and the formation and the decay of  $\text{Ag}_1^0(\text{CN})_2^{2-}$ . However, the absorption at 450 and 500 nm increases quickly up to 100 ns (Figure 2). This observation means that the extinction coefficient of the complexed atom is higher than that of  $e_{\text{hyd}}^-$  at these two wavelengths (around  $4000 \text{ L}\cdot\text{mol}^{-1}\cdot\text{cm}^{-1}$  and  $6000 \text{ L}\cdot\text{mol}^{-1}\cdot\text{cm}^{-1}$  respectively).

The silver redox couple involved in the first reduction step (8) is  $\text{Ag}(\text{CN})_2^-/\text{Ag}_1^0(\text{CN})_2^{2-}$ . It has been observed recently that the propanol-2 radical ( $-2 V_{\text{NHE}}$  at pH = 10) which reduces  $\text{Ag}^+$  into  $\text{Ag}_1^0$  does not reduce  $\text{Ag}(\text{CN})_2^-$ .<sup>21,27</sup> This was explained by the fact that cyanide ligands lower the redox potential of  $\text{Ag}(\text{CN})_2^-/\text{Ag}_1^0(\text{CN})_2^{2-}$  down to  $-2.6 V_{\text{NHE}}$ , according to the theoretical calculation.<sup>20</sup>

The spectrum of  $\text{Ag}_1^0(\text{CN})_2^{2-}$  (absorbing at 450 and 500 nm) is then significantly different from that of hydrated  $\text{Ag}_1^0$ . The presence of cyanide ligands induces a red shift of the silver atom spectrum assigned to a charge transfer to solvent (CTTS), and the appearance of an additional absorption band which is probably due to metal-ligand-charge-transfer (MLCT). Such an absorption band, due to interaction with the ligands, has already been observed in the presence of ammonia.<sup>19</sup>

**Second Step 100–300 ns.** After 100 ns, the two absorption bands of  $\text{Ag}_1^0(\text{CN})_2^{2-}$  begin to decrease (Figures 1 and 2), while the 350 nm absorption band continues to grow up to 300 ns (Figures 1 and 3). We have shown, in previous work,<sup>20</sup> that the dissociation of  $\text{Ag}_1^0(\text{CN})_2^{2-}$  into  $\text{Ag}_1^0 + 2\text{CN}^-$  is thermodynamically impossible in aqueous solution. On the other hand, the species formed during the decay of  $\text{Ag}_1^0(\text{CN})_2^{2-}$  displays more than a single absorption band at 350 nm. Thus, this latter band is not due to the naked silver atom but, similarly to what is known in free aqueous medium, this peak must be assigned to the species  $\text{Ag}_2^+$  complexed by  $\text{CN}^-$ . Since we do not know exactly the number of  $\text{CN}^-$  bound to  $\text{Ag}_2^+$ , this species is denoted  $(\text{Ag}_2^+, \text{CN}^-)$ . It is formed during the decay of  $\text{Ag}_1^0(\text{CN})_2^{2-}$  according to



When  $\text{Ag}_1^0(\text{CN})_2^{2-}$  decreases, a new absorption band appears at 410 nm as early as 200 ns (Figure 1). In addition, when the two bands of  $\text{Ag}_1^0(\text{CN})_2^{2-}$  have disappeared at 900 ns, a residual absorption is still present at 490 nm. At this latter time, the

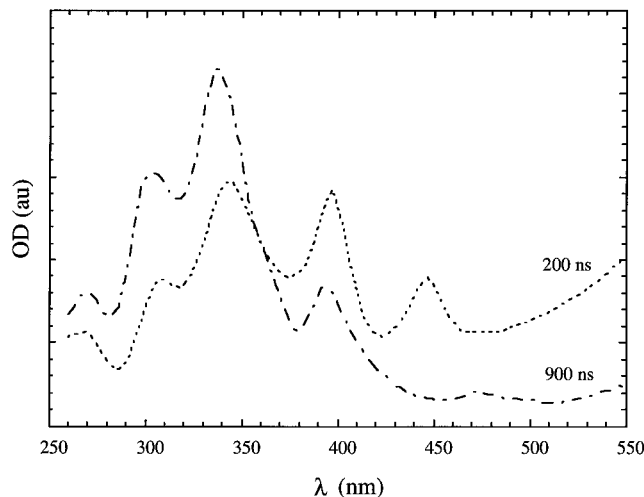


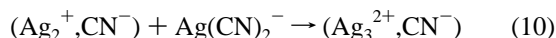
**Figure 4.** Spectra obtained by pulse radiolysis of a solution containing  $[\text{Ag}^+] = 10^{-3} \text{ mol}\cdot\text{L}^{-1}$ ,  $[\text{EDTA}] = 5 \times 10^{-3} \text{ mol}\cdot\text{L}^{-1}$ , and  $[2\text{-propanol}] = 0.2 \text{ mol}\cdot\text{L}^{-1}$ , 200 and 900 ns after the pulse. The pH was adjusted at 10.

spectrum presents three absorption bands at wavelengths higher than 300 nm (Figure 1). These three peaks (350, 410, and 490 nm) display the same kinetic evolution after 900 ns and thus characterize the same species, namely  $(\text{Ag}_2^+, \text{CN}^-)$ .

The spectrum of  $(\text{Ag}_2^+, \text{CN}^-)$  is thus composed of three absorption bands at 350, 410, and 490 nm which decrease together after 300 ns; this results from the fact that the following species do not absorb in the visible range of the spectrum. In the absence of cyanide ligands,  $\text{Ag}_2^+$  presents two absorption bands at 260 and 310 nm.<sup>6</sup> The presence of  $\text{CN}^-$  induces, as it does for the atom, the red shift of the spectrum of  $\text{Ag}_2^+$  and the appearance of a third band assigned once again to the interaction of the metallic core with the complexing agent.

The rate constant ( $k_9 = 1 \times 10^{10} \text{ L}\cdot\text{mol}^{-1}\cdot\text{s}^{-1}$ ) of reaction 9 is estimated from the pseudo-first-order analysis of the absorption buildup at 350 nm (at this wavelength, the absorption of  $\text{Ag}_1^0(\text{CN})_2^{2-}$  can be neglected). This value is close to that found in the absence of ligands ( $k_4 = 8.5 \times 10^9 \text{ L}\cdot\text{mol}^{-1}\cdot\text{s}^{-1}$ ).<sup>4</sup> The disappearance of  $\text{Ag}_1^0(\text{CN})_2^{2-}$  through reaction 9 is then faster than its formation. Thus, the concentration of the complexed atom remains low and we understand easily the early presence of  $(\text{Ag}_2^+, \text{CN}^-)$  absorption bands in the spectrum (Figure 1).

**Third Step after 300 ns.** During this step, the three bands of  $(\text{Ag}_2^+, \text{CN}^-)$  decrease while the absorption at 270 nm, due to the formation of the subsequent species (supposed to be, as in free medium,<sup>7</sup>  $(\text{Ag}_4^{2+}, \text{CN}^-)$  and/or  $(\text{Ag}_3^{2+}, \text{CN}^-)$ ), grows up to 700 ns (Figure 3) through the two reactions



The subsequent steps, not studied in this work, lead to larger clusters complexed by cyanide.<sup>27</sup>

**II. EDTA Complexing Effect. Transient Spectra.** Figure 4 shows the spectra obtained at two times after the pulse: 200 and 900 ns. At 200 ns, on the red side of the spectrum, the broad band of the hydrated electron is clearly present while two narrow bands have appeared peaking at 400 and 450 nm. After 200 ns, the absorption decays quickly at these two wavelengths. Other bands are present in the range 250–350 nm but continue to increase after 200 ns (Figure 4).

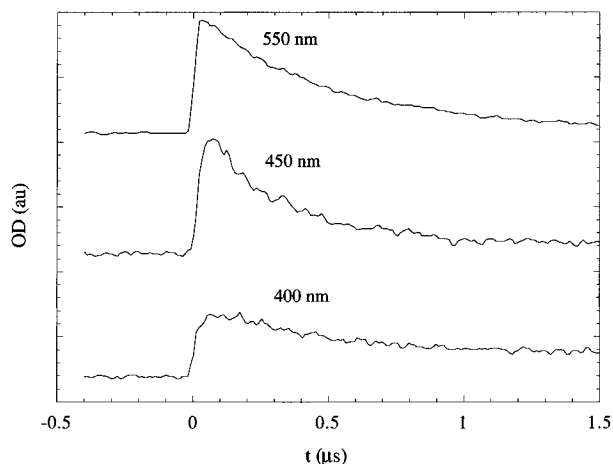


**Figure 5.** Time profile of the absorption at 550, 450, and 400 nm. Same conditions as Figure 4.

At 900 ns, the absorption of the hydrated electron and the band at 450 nm have completely faded. The bands at 300 and 340 nm are fully developed. An absorption is still present at 400 nm (Figure 4).

After 900 ns, the absorption at 270 nm continues to increase up to 1.5  $\mu$ s.

**Kinetic Steps.** In order to distinguish more clearly the successive reactions, the time profile of absorbances has been plotted in Figures 5 and 6 for typical wavelengths: over the first 900 ns, two main kinetic steps can be seen which are then followed by several others.

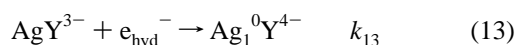
**First Step 0–125 ns.** The initial absorption in the red part of the spectrum is due to  $e_{\text{hyd}}^-$  (Figure 4) and decays (Figure 5 at 550 nm) according to pseudo-first-order kinetics. The reduction of  $\text{AgY}_3^-$  by  $e_{\text{hyd}}^-$  may lead to two different products, viz.  $\text{Ag}_1^0\text{Y}^{4-}$  or  $\text{Ag}_1^0 + \text{Y}^{4-}$ . Since two peaks appear at 400 and 450 nm and no absorption maximum is observed at 360 nm during the electron decay (Figure 4), we conclude that these bands belong to the product of the reduction of  $\text{AgY}_3^-$  by the hydrated electron which is the complexed atom  $\text{Ag}_1^0\text{Y}^{4-}$  and not the free silver atom  $\text{Ag}_1^0$ . The spectrum of  $\text{Ag}_1^0\text{Y}^{4-}$  is significantly different from that of  $\text{Ag}_1^0$  and  $\text{Ag}_1^0(\text{CN})_2^{2-}$ . The presence of EDTA induces, as does the cyanide ligand, a red shift of the spectrum of the silver atom and the appearance of an additional absorption band which is probably due to a metal-to-ligand charge transfer (MLCT). However, the two absorption bands of the complexed atom are more strongly red-shifted in the case of  $\text{CN}^-$  which is a stronger complexing agent than  $\text{Y}^{4-}$ .

At 400 and 450 nm, the absorption increases quickly after the pulse (Figure 5). This observation means that the extinction coefficient of the complexed atom is higher than that of  $e_{\text{hyd}}^-$  at these two wavelengths.

We have studied the atom formation by analyzing the electron decay at 550 nm (Figure 5). Taking into account the following reaction<sup>28</sup>



we can deduce the value of the rate constant of reaction 13:



The equation corresponding to the electron decay can be solved only if  $\text{AgY}_3^-$  is in excess in regard to  $e_{\text{hyd}}^-$ . Then, this differential equation displays a general solution:

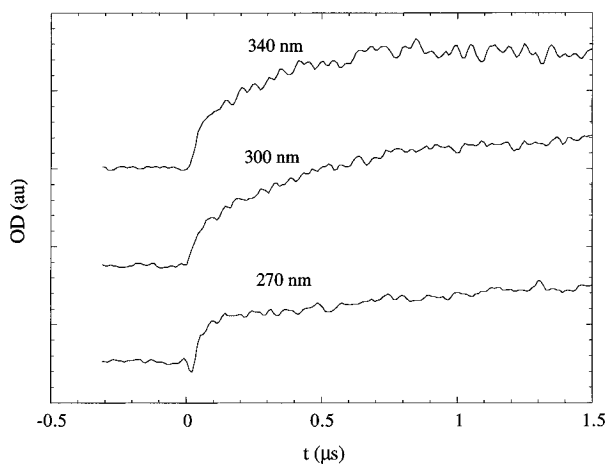


**Figure 6.** Time profile of the absorption at 340, 300, and 270 nm. Same conditions as Figures 4 and 5.

$$[e_{\text{hyd}}^-]_t = \frac{\exp(-k_{\text{obs}}t)}{\frac{2k_{12}}{k_{\text{obs}}}[-\exp(-k_{\text{obs}}t) + 1] + \frac{1}{[e_{\text{hyd}}^-]_{t=0}}} \quad (\text{eq 1})$$

where

$$k_{\text{obs}} = k_{13}[\text{AgY}_3^-]_{t=0} \quad (\text{eq 2})$$

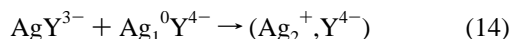
and where  $[e_{\text{hyd}}^-]_t$  is the electron concentration at time  $t$  (in particular,  $[e_{\text{hyd}}^-]_{t=0}$  is the initial concentration).

We have plotted the time evolution of the electron by adjusting the value of  $k_{13}$  to reproduce the experimental decay (Figure 5). The value of  $k_{13}$  which allows the superposition of the calculated and experimental evolutions amounts to  $k_{13} = 1.7 \times 10^9 \text{ L} \cdot \text{mol}^{-1} \cdot \text{s}^{-1}$  and is close to the value found by Anbar.<sup>26</sup> This value has to be compared with the rate constant  $3.6 \times 10^{10} \text{ L} \cdot \text{mol}^{-1} \cdot \text{s}^{-1}$  obtained in the absence of EDTA.<sup>8</sup> The reaction rate is much lower in the presence of EDTA because of the change in the effective charge of the complexed silver ion.

**Second Step, up to 900 ns.** The optical density increases at 300 and 340 nm (Figure 6) during the decay of  $\text{Ag}_1^0\text{Y}^{4-}$  at 400 and 450 nm (Figure 5). At 400 nm, the complexed atom absorbs, but after the decay of  $\text{Ag}_1^0\text{Y}^{4-}$  (well observed at 450 nm), an important residual absorption remains.

After the decrease of  $\text{Ag}_1^0\text{Y}^{4-}$ , three bands are observed at 310, 340, and 400 nm (Figure 4). Similarly to what is known in the presence of cyanide ligands, these peaks must be assigned to the species  $\text{Ag}_2^+$ , which reveals to be itself complexed with EDTA ( $\text{Ag}_2^+$ ,  $\text{Y}^{4-}$ ). The presence of EDTA induces, as does  $\text{CN}^-$ , the red shift of the spectrum of  $\text{Ag}_2^+$  and the appearance of a third band assigned once again to the interaction of the metallic core with the complexing agent. However, the red shift is less marked than in the case of cyanide. Note that we do not know exactly the number of  $\text{Y}^{4-}$  bound to  $\text{Ag}_2^+$ . The spectral time evolution displays an isosbestic point at 355 nm which indicates that  $\text{Ag}_1^0\text{Y}^{4-}$  and ( $\text{Ag}_2^+$ ,  $\text{Y}^{4-}$ ) have the same extinction coefficient at this wavelength.

The rate constant of ( $\text{Ag}_2^+$ ,  $\text{Y}^{4-}$ ) formation is estimated from the pseudo-first-order analysis of the absorption buildup at 340 nm (at this wavelength the absorption of  $\text{Ag}_1^0\text{Y}^{4-}$  and of the species issued from the decay of ( $\text{Ag}_2^+$ ,  $\text{Y}^{4-}$ ) can be neglected). Analyzing the pseudo-first-order rate constant  $k_{\text{obs}}$  as a function of  $\text{Ag}^+$  concentration and keeping the initial ratio  $[\text{EDTA}]/[\text{Ag}^+]$  constant leads to a linear plot. We obtain  $k_{14} = 1.6 \times 10^9 \text{ L} \cdot \text{mol}^{-1} \cdot \text{s}^{-1}$  for the following process:



This value is lower than in the absence of ligands  $k_4 = 8.5 \times 10^9 \text{ L} \cdot \text{mol}^{-1} \cdot \text{s}^{-1}$ .<sup>7</sup>

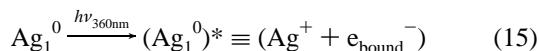
After 900 ns, the main change is the growth of the absorption at 270 nm (Figure 6) due to the formation of the subsequent species (supposed to be  $(\text{Ag}_3^{2+}, \text{Y}^{4-})$  and/or  $(\text{Ag}_4^{2+}, \text{Y}^{4-})$ ).

## Discussion

**Spectra and Redox Behavior.** The presence of the  $\text{CN}^-$  ligand induces the lowering of the redox potential of the silver monomeric couple and the red shift of the absorption spectrum of the silver atom. We try here to correlate these two effects through the complexing strength of the cyanide ligand.

The absorption process of light may induce the detachment of an electron with subsequent localization in a solvent cavity.<sup>30</sup> Then the electron is bound within a stationary state higher than that required for ionization ( $e_{\text{bound}}^-$ ).<sup>31</sup> This class of transitions is called charge transfer to solvent (CTTS). The corresponding spectra are therefore a special example of electron-transfer spectra<sup>31-33</sup> and are known to depend on the solvent, temperature, and pressure.<sup>32</sup> Since the solvent plays such an integral part in defining the excited CTTS state, the spectra provide information concerning the structure of the medium surrounding the ion.

Actually,  $\text{Ag}_1^0$ -solvent interaction looks rather like that of an  $\text{Ag}^+$  core plus one negative charge mostly delocalized on the surrounding solvent molecules, thus supporting the CTTS structure put forward by Kevan.<sup>17</sup> In addition, the wavelength maximum of the optical transition of  $\text{Ag}_1^0$ , solvated in various environments, shifts markedly according to the polarity of the solvent,<sup>18,34</sup> as does also the spectrum of the solvated electron,<sup>35</sup> and according to the temperature.<sup>34</sup> As for halide anions,<sup>31,32</sup> the process of light absorption corresponding to the CTTS spectrum of  $\text{Ag}_1^0$  can be written



where  $(\text{Ag}_1^0)^*$  is the excited CTTS state and  $h\nu_{360\text{nm}} = hc/\lambda_{\text{max}}$  is the energy corresponding to the maximum absorption of the CTTS band of  $\text{Ag}_1^0$ .

The continuum model considers the binding energy of  $e_{\text{bound}}^-$  in the CTTS state as due partly to the persistent polarization of the medium and partly to the electronic polarization induced by the electron in its excited state. In this state, the electron is on the average fairly removed from  $\text{Ag}^+$ , so that the effect of the latter on the binding energy could be neglected.<sup>31</sup>

$(\text{Ag}_1^0)^*$  undergoes a strong coupling with the solvent as a positive solvated core surrounded by a negative charge delocalized over the neighboring polar molecules. The excited state of the CTTS transition  $(\text{Ag}_1^0)^*$  is 3.5 eV (360 nm) above the ground state, while  $\text{Ag}^+$  lies above  $\text{Ag}_1^0$  by the ionization potential in solution  $IP_{\text{sol}} = 2.6 \text{ eV}$ <sup>5</sup> (Figure 7). Thus the excited state  $(\text{Ag}_1^0)^*$  is autoionizing by 0.8 eV,<sup>34</sup> whereas the ground state  $\text{Ag}_1^0$  is not. This excess energy corresponds to the difference between the solvent reorganization energies around the two systems  $\text{Ag}^+$  and  $(\text{Ag}_1^0)^*$ .

**$\text{CN}^-$  Effect.** The complexed  $\text{Ag}_1^0(\text{CN})_2^{2-}$  atom is autoionizing in the gas phase, but not in aqueous solution.<sup>20</sup> Its spectrum presents two absorption bands at 450 and 500 nm. One of these is a CTTS absorption band while the other is attributed to a MLCT transition. Since the cyanide ligands are closer to the metal core than the solvent molecules and since the ligands are negatively charged, it seems that the CTTS transition (transition to the solvent) is more energetic than the

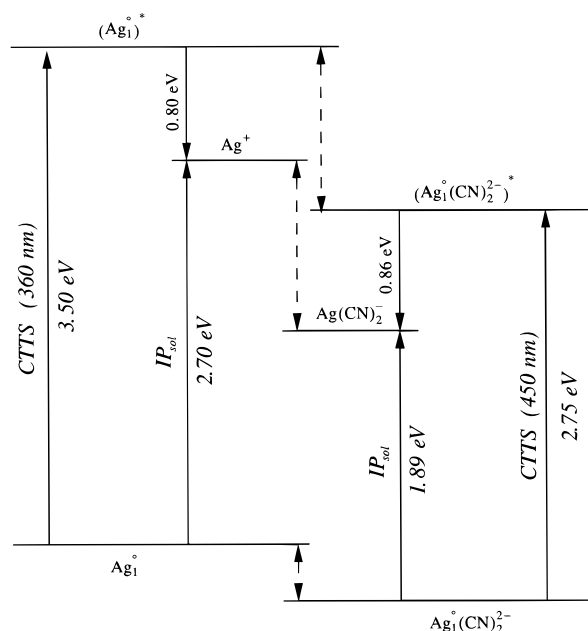
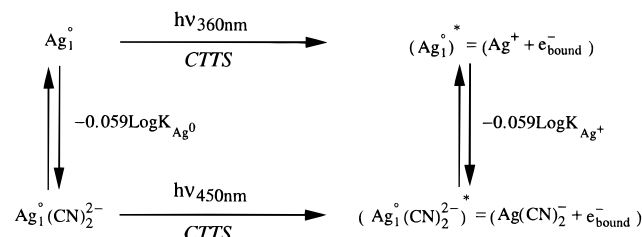


**Figure 7.** Energy levels of silver atom and silver ion in aqueous solution in the presence and absence of cyanide.

MLCT one (transition to the ligands). The 450 and 500 nm absorption bands are therefore attributed respectively to the CTTS and MLCT transitions. Thus, the free and cyanide-complexed silver atom spectra present a CTTS absorption band at 360 and 450 nm, respectively: the experimental spectrum shift amounts to +90 nm.

Figure 7 displays the energy levels of both the silver atom and silver ion in aqueous solution in the presence and in the absence of cyanide ligands. Note that the difference between the energies of  $\text{Ag}_1^0(\text{CN})_2^{2-}$  and  $\text{Ag}_1^0$  in solution amounts to 0.41 eV.<sup>20</sup> The CTTS absorption at 450 nm (2.75 eV) corresponds to the excitation of  $\text{Ag}_1^0(\text{CN})_2^{2-}$  to  $(\text{Ag}_1^0(\text{CN})_2^{2-})^* \equiv (\text{Ag}(\text{CN})_2^- + e_{\text{bound}}^-)$ . This transition, as in the absence of cyanide, is more energetic than the ionization potential in solution of  $\text{Ag}_1^0(\text{CN})_2^{2-}$  (1.89 eV<sup>20</sup>). In this case, the binding energy of the electron amounts to 0.86 eV instead of 0.8 eV in free aqueous medium. Thus, it seems that this excess energy does not depend greatly on the presence of cyanide, showing that the electron is delocalized almost in the same way around  $\text{Ag}^+$  and  $\text{Ag}(\text{CN})_2^-$ . The difference between the energies of  $\text{Ag}(\text{CN})_2^-$  and  $\text{Ag}^+$  (1.22 eV) is then close to the difference between the energies of  $(\text{Ag}_1^0(\text{CN})_2^{2-})^* \equiv (\text{Ag}(\text{CN})_2^- + e_{\text{bound}}^-)$  and  $(\text{Ag}_1^0)^* \equiv (\text{Ag}^+ + e_{\text{bound}}^-)$  (Figure 7): the complexation constant of  $(\text{Ag}_1^0)^*$  by cyanide ligands is close to that of  $\text{Ag}^+$ .

Hence, according to the continuum model,<sup>31</sup> we may assume that the electron is fairly removed from free and complexed silver ions so that the effect of the presence of cyanide on the binding energy of the electron could be neglected. Let us write a thermodynamic cycle



including the CTTS transitions with (450 nm) and without (360 nm) cyanide ligands and including the two complexation equilibria of  $\text{Ag}^+$  and  $\text{Ag}_1^0$  by cyanide. The complexation

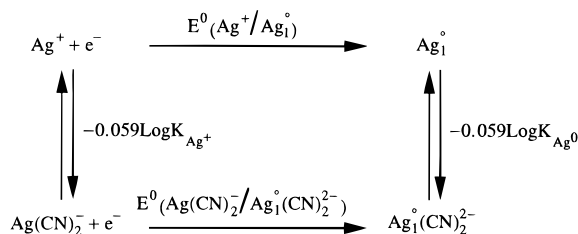
constants of  $\text{Ag}^+$  and  $\text{Ag}_1^0$  by cyanide are denoted  $K_{\text{Ag}^+}$  and  $K_{\text{Ag}^0}$  and amount to  $10^{20.7}$  and  $10^7$ , respectively.<sup>20</sup>

Then, if we assume that the value of the complexation constant of the silver atom ( $\text{Ag}_1^0$ )\* in its excited state is close to that of the silver ion  $\text{Ag}^+$  in its ground state ( $K_{\text{Ag}^+}$ ), we can write

$$h\nu_{450\text{nm}} - h\nu_{360\text{nm}} = 0.059(\log K_{\text{Ag}^0} - \log K_{\text{Ag}^+}) \quad (\text{eq } 3)$$

Now we can expect theoretically a spectral shift  $\Delta\lambda$  between the absorption maxima of  $\text{Ag}_1^0$  and  $\text{Ag}_1^0(\text{CN})_2^{2-}$  which amounts to +110 nm, close to the experimental shift (+90 nm).

On the other hand, a second thermodynamic cycle



including the two redox potentials  $E^0$  (of the couples  $\text{Ag}^+/\text{Ag}_1^0$  and  $\text{Ag}(\text{CN})_2^-/\text{Ag}_1^0(\text{CN})_2^{2-}$ ) and the two complexation equilibria (of  $\text{Ag}^+$  and  $\text{Ag}_1^0$  by cyanide ligands) gives<sup>20</sup>

$$|e|E^0(\text{Ag}(\text{CN})_2^-/\text{Ag}_1^0(\text{CN})_2^{2-}) - |e|E^0(\text{Ag}^+/\text{Ag}_1^0) = 0.059(\log K_{\text{Ag}^0} - \log K_{\text{Ag}^+}) \quad (\text{eq } 4)$$

If the silver ion is more strongly complexed by cyanide ligands than the silver atom, the CTTS band of the atom is red shifted (eq 3) and at the same time, the redox potential of the monomeric couple is lowered (eq 4). Regarding eqs 3 and 4, the red shift of the CTTS band, which is more pronounced when the ligand interaction is stronger, may be correlated with the redox potential decrease toward negative values. This correlation provides a means for deriving, from experimental spectral shifts, thermodynamic information (on complexation constants and redox potentials) which would be hard to obtain directly for transient clusters.

From eqs 3 and 4, considering  $E^0(\text{Ag}^+/\text{Ag}_1^0) = -1.75 \text{ V}_{\text{NHE}}$  and  $\Delta\lambda = 90 \text{ nm}$  (the experimental value), we obtain

$$E^0(\text{Ag}(\text{CN})_2^-/\text{Ag}_1^0(\text{CN})_2^{2-}) = -2.5 \text{ V}_{\text{NHE}} \quad (\text{eq } 5)$$

which is very close to the value  $-2.6 \text{ V}_{\text{NHE}}$  estimated theoretically.<sup>20</sup>

**EDTA Effect.** Similarly the experimental shift of the spectrum of the atom in the presence of EDTA allows the estimation of the redox potential of the thermodynamic couple  $\text{AgY}^{3-}/\text{Ag}_1^0\text{Y}^{4-}$ . The more energetic transition in the case of  $\text{Ag}_1^0\text{Y}^{4-}$  is again the CTTS one at 400 nm. The CTTS absorption band is thus red shifted in the presence of EDTA by an experimental value of 40 nm. This shift is smaller than that observed in the presence of cyanide. This can be understood in terms of difference in the complexing strength of the silver atom by the two ligands with the aid of eq 3. Since the complexation constant of  $\text{Ag}^+$  by  $\text{Y}^{4-}$  amounts to  $10^{7.3}$ <sup>23</sup> and since  $\Delta\lambda = 40 \text{ nm}$  (experimental value), the complexation constant of  $\text{Ag}_1^0$  by  $\text{Y}^{4-}$  is  $10^{1.4}$ . This value is much smaller than that of  $\text{Ag}_1^0$  by the cyanide ligands ( $10^7$ <sup>20</sup>).

Now, we may estimate the redox potential of  $\text{AgY}^{3-}/\text{Ag}_1^0\text{Y}^{4-}$  by means of eqs 3 and 4:

$$E^0(\text{AgY}^{3-}/\text{Ag}_1^0\text{Y}^{4-}) = -2.2 \text{ V}_{\text{NHE}} \quad (\text{eq } 6)$$

As in the case of cyanide ligands, this redox potential is higher than that of the hydrated electron but lower than that of the propanol-2 radical. The redox potential of the monomeric couple is lower in the presence of cyanide than in the presence of EDTA. This again can be understood in terms of complexing effects (eq 4): cyanide is a stronger complexing agent than  $\text{Y}^{4-}$ .

## Conclusion

The present paper shows the strong complexation effect of ligands on the kinetics, spectral properties, and redox properties of metal clusters. We have shown by pulse radiolysis experiments that the complexation of silver ions by  $\text{CN}^-$  or EDTA ( $\text{Y}^{4-}$  in basic medium) decreases the formation rate of silver atoms. On the other hand,  $\text{Ag}_1^0$  and  $\text{Ag}_2^+$  have been found to be complexed by  $\text{CN}^-$  and  $\text{Y}^{4-}$  and their transient absorption spectra have been determined. In addition to the usual charge-transfer-to-solvent (CTTS) bands which have been found to be red shifted in the presence of ligands, the spectra of the early clusters exhibit an additional band assigned to a metal–ligand transition. We have therefore proposed a correlation between the red shift of the CTTS band, which is more pronounced when the ligand interaction is stronger, and the redox potential decrease. This correlation provides a means to derive, from experimental spectral shifts, thermodynamic information: the redox potentials of  $\text{AgY}^{3-}/\text{Ag}_1^0\text{Y}^{4-}$  and  $\text{Ag}(\text{CN})_2^-/\text{Ag}_1^0(\text{CN})_2^{2-}$  have been estimated respectively at  $-2.2 \text{ V}_{\text{NHE}}$  and  $-2.5 \text{ V}_{\text{NHE}}$ . This latter value agrees with previous theoretical calculation.

To check the validity of such a correlation, it would be interesting to evaluate theoretically, as in the case of  $\text{CN}^-$ , the redox potential  $E^0(\text{AgY}^{3-}/\text{Ag}_1^0\text{Y}^{4-})$  and to test experimentally the reactivity of  $(\text{CH}_3)_2\dot{\text{C}}\text{OH}$  toward  $\text{AgY}^{3-}$ . In addition,  $\text{Ag}_1^0$  and  $\text{Ag}_2^+$  systems should be addressed in the presence of other ligands and this work is in progress. In the absence of metal particles or impurities, only extremely strong electron donors, like the hydrated electrons, can reduce  $\text{AgY}^{3-}$  and  $\text{Ag}(\text{CN})_2^-$  to  $\text{Ag}_1^0\text{Y}^{4-}$  and  $\text{Ag}_1^0(\text{CN})_2^{2-}$ , respectively. This marked stability of the two complexes in aqueous solution toward reduction is due to the protection of the  $\text{Ag}^+$  ion by the two complexing agents  $\text{Y}^{4-}$  and  $\text{CN}^-$ .

## References and Notes

- (1) Baxendale, J. H.; Fielden, E. M.; Keene, J. P. *In Pulse Radiolysis*; Academic Press: London, 1965; p 207.
- (2) Pukies, J.; Roebke, W.; Henglein, A. *Ber. Bunsen-Ges. Phys. Chem.* **1968**, 72, 842.
- (3) Tausch-Treml, R.; Henglein, A.; Lilie, J. *Ber. Bunsen-Ges. Phys. Chem.* **1978**, 82, 1335.
- (4) Henglein, A.; Tausch-Treml, R. *J. Colloid Interf. Sci.* **1981**, 80, 84.
- (5) Mostafavi, M.; Marignier, J. L.; Amblard, J.; Belloni, J. *Radiat. Phys. Chem.* **1989**, 34, 605.
- (6) Ershov, B. G.; Janata, E.; Henglein, A.; Fojtik, A. *J. Phys. Chem.* **1993**, 97, 4589.
- (7) Janata, E.; Henglein, A.; Ershov, B. G. *J. Phys. Chem.* **1994**, 98, 10888.
- (8) Beaumont, P. C.; Powers, E. L. *Int. J. Radiat. Biol. Relat. Stud. Phys. Chem. Med.* **1983**, 43, 485.
- (9) Mostafavi, M.; Keghouche, N.; Delcourt, M. O.; Belloni, J. *Chem. Phys. Lett.* **1990**, 167, 193.
- (10) Mostafavi, M.; Keghouche, N.; Delcourt, M. O. *Chem. Phys. Lett.* **1990**, 169, 81.
- (11) Henglein, A.; Linnert, T.; Mulvaney, P. *Ber. Bunsen-Ges. Phys. Chem.* **1990**, 94, 1449.
- (12) Mostafavi, M.; Delcourt, M. O.; Picq, G. *Radiat. Phys. Chem.* **1993**, 41, 453.
- (13) Rémita, S.; Orts, J. M.; Feliu, J. M.; Mostafavi, M.; Delcourt, M. O. *Chem. Phys. Lett.* **1994**, 218, 115.
- (14) Mostafavi, M.; Delcourt, M. O.; Keghouche, N.; Picq, G. *Radiat. Phys. Chem.* **1992**, 40, 453.
- (15) Ershov, B. G.; Janata, E.; Henglein, A. *J. Phys. Chem.* **1993**, 97, 339.
- (16) Farhatziz; Cordier, P.; Perkey, L. M. *Radiat. Res.* **1976**, 68, 23.

- (17) Kevan, L. *J. Phys. Chem.* **1981**, 85, 1628.
- (18) Belloni, J.; Delcourt, M. O.; Marignier, J. L.; Amblard, J. *Radiation Chemistry*; Hedwig, P., Nyikos, L., Schiller, R., Eds.; Akademia Kiado: Budapest, 1987; p 89.
- (19) Texier, I.; Remita, S.; Archirel, P.; Mostafavi, M. *J. Phys. Chem.*, in press (1996).
- (20) Rémita, S.; Archirel, P.; Mostafavi, M. *J. Phys. Chem.* **1995**, 99, 13198.
- (21) Texier, I.; Mostafavi, M. *Radiat. Phys. Chem.* submitted for publication (1996).
- (22) Ringbom, A. *Les complexes en chimie analytique*; Dunod: Paris, 1967.
- (23) Rémita, S.; Mostafavi, M.; Delcourt, M. O. *New J. Chem.* **1994**, 18, 581.
- (24) Bielski, B. H. J.; Allen, A. O. *J. Am. Chem. Soc.* **1977**, 99, 5931.
- (25) Buitenhuis, R.; Bakker, C. M. N.; Stock, F. R.; Louwrier, P. W. F. *Radiochim. Acta* **1977**, 24, 189.
- (26) Anbar, M.; Hart, E. J. *J. Phys. Chem.* **1965**, 69, 973.
- (27) De Cointet, C. Thèse de Doctorat, Université Paris XI, Orsay, 1994.
- (28) Gordon, S.; Hart, E. J.; Matheson, M. S.; Rabani, J.; Thomas, J. K. *J. Am. Chem. Soc.* **1963**, 85, 1375.
- (29) Mostafavi, M. Thèse de Doctorat, Université Paris XI, Orsay, 1989.
- (30) Staib, A.; Borgis, D. *J. Chem. Phys.* **1995**, 103, 2642.
- (31) Treinin A., *J. Phys. Chem.* **1964**, 68, 893.
- (32) Blandamer, M. J.; Fox, M. F. *Chem. Rev.* **1970**, 59.
- (33) Grossweimer, L. I.; Matheson, M. S. *J. Phys. Chem.* **1957**, 61, 1089.
- (34) Belloni, J.; Khatouri, J.; Mostafavi, M.; Amblard, J. *Ultrafast Reaction Dynamics and Solvent Effects*, AIP Conference Proceedings 298; AIP Press: New York, 1994; p 107.
- (35) Belloni, J.; Marignier, J. L. *Radiat. Phys. Chem.* **1989**, 34, 157.

JP960176G